**Atmospheric
Chemistry
and Physics
Discussions**

ACPD

6, 12503–12548, 2006

TORCH2
hygroscopicity
closure

M. Gysel et al.

Title Page

Abstract	Introduction
Conclusions	References
Tables	Figures

|ı◀|▶ı|
|◀|▶|

| Back | Close |

Full Screen / Esc

Printer-friendly Version

Interactive Discussion

EGU

Closure between measured and modelled particle hygroscopic growth during TORCH2 implies ammonium nitrate artefact in the HTDMA measurements

M. Gysel[1,2], J. Crosier[1], D. O. Topping[1], J. D. Whitehead[1], K. N. Bower[1],
M. J. Cubison[1,*], P. I. Williams[1], M. J. Flynn[1], G. B. McFiggans[1], and H. Coe[1]

[1]Atmospheric Sciences Group, SEAES, University of Manchester, P.O. Box 88, Manchester, M60 1QD, UK
[2]Labor für Atmsphärenchemie, Paul Scherrer Institut, 5232 Villigen PSI, Switzerland
[*]now at: Cooperative Institute for Research in Environmental Sciences, University of Colorado, Boulder, CO 80309, USA

Correspondence to: M. Gysel (martin.gysel@psi.ch)

EGU

Abstract

Measurements of aerosol properties were made in aged polluted and clean background air masses encountered at the North Norfolk (UK) coastline during the second field campaign of the Tropospheric ORganic CHemistry project (TORCH2) in May 2004. Hygroscopic growth factor (GF) measurements were performed at 90% relative humidity (RH) for D_0 =27–217 nm particles using a Hygroscopicity Tandem Differential Mobility Analyser (HTDMA), while the aerosol composition was simultaneously measured with an Aerodyne aerosol mass spectrometer (Q-AMS). During the clean background events the aerosol was characterised by little size dependence of properties with generally large GFs and inorganic sulphate being the dominant compound. In aged polluted air masses the particles were dominated by inorganic sulphate and nitrate at larger sizes, whereas organics were the largest fraction in smaller particles, thus explaining the trend of smaller GFs at smaller sizes. Organics do contribute to the hygroscopic growth, particularly at small sizes, but generally the dominant contribution to growth at 90% RH comes from inorganic salts. The ZSR mixing rule was used to predict GFs based on the chemical composition, theoretical GFs of pure inorganic salts and a "bulk" GF of ∼1.20 for the organics. Good quantitative closure with HTDMA measurements as a function of both particle size and time was achieved in the absence of nitrate. However, GFs were clearly overpredicted at times when a significant fraction of nitrate was present. After careful considerations we attribute the overprediction to substantial evaporation losses of ammonium nitrate in the HTDMA instrument. If true, this implies that the ZSR predictions based on composition might be more representative of the actual "bulk" behaviour of undisturbed ambient particles than the HTDMA measurements.

The simplified model approach using the ZSR rule and a constant organic growth factor made high size and time resolution possible, which has proven to be essential for a valid closure study. The ZSR mixing rule appears to be sufficiently accurate, as the GF predictions are more sensitive to the exact GFs of the inorganic compounds than

to the growth factor of the moderately hygroscopic organics. Therefore a more detailed analysis and modelling of the organic fraction at the expense of time and size resolution is not worth the effort for an aged aerosol and discrepancies in either direction might even be cancelled out by averaging.

1   Introduction

Atmospheric aerosols have many effects on the environment. The most readily perceived is visibility degradation (Hand et al., 2002). The Earth's climate is also affected because aerosol particles scatter and absorb solar radiation (direct aerosol effect; Kay and Box, 2000) and because they alter the formation and precipitation efficiency of clouds, thereby causing the so-called indirect aerosol radiative effect associated with these changes in cloud properties and lifetime (Ramanathan et al., 2001). Hygroscopic properties of atmospheric particles are important for the aforementioned effects, since light scattering properties and cloud condensation nuclei (CCN) activity strongly depend on the relative humidity (RH) dependent particulate water content.

The ability of a particle to absorb water depends on its composition. Inorganic salts, organic matter, elemental carbon and mineral dust are major aerosol components and have been investigated in pure and mixed form in numerous studies (Weingartner et al., 1997; Gysel et al., 2002; Hämeri et al., 2002; Wise et al., 2003; Vlasenko et al., 2005). In the laboratory the hygroscopic behaviour of particles is reasonably well understood, and semi-empirical models predicting hygroscopic growth factors of multicomponent inorganic/organic particles are also available (ADDEM;Topping et al., 2005a; Topping et al., 2005b).

In so-called "hygroscopicity closure" studies one tries to predict hygroscopic growth factors of aerosol particles based on their chemical composition. Achieving this goal is complicated for atmospheric particles, because their composition typically depends on particle size, differs between individual particles, varies with time, and often comprises a vast number of different organic species. In earlier studies only the contribution of

TORCH2 hygroscopicity closure

M. Gysel et al.

EGU

the inorganic aerosol fraction was predicted, and the unexplained water uptake was just attributed to the organic fraction. In this way it has been found that the organic aerosol fraction does most likely contribute to hygroscopic growth (Saxena et al., 1995; Swietlicki et al., 1999; Dick et al., 2000; Weingartner et al., 2004), except for some studies of fresh urban particles, in which the organics rather appear to be inert with respect to water uptake (Saxena et al., 1995; Berg et al., 1998). These findings have been confirmed with a closure using extracts of the organic and the total water-soluble fraction from ambient filter samples (Gysel et al., 2004).

A detailed closure study has been done by McFiggans et al. (2005), where they used a combination of impactor and aerosol mass spectrometer (Q-AMS) measurements to obtain size-resolved composition needed as input for ADDEM predictions of growth factors. By comparison with Hygroscopicity Tandem Differential Mobility Analyser (HT-DMA) measurements of growth factors it was found that the variability in growth factor was largely dominated by the inorganic:organic mass ratio at any given size and that the water associated with the organic fraction was modest and relatively invariant between organics of different ensemble functional representations at two comparable locations. Full multicomponent model calculations using ADDEM are demanding and determining the functional representation of the organic aerosol fraction is very costly and a limiting factor for both time and size resolution of the chemical analysis. Therefore McFiggans et al. (2005) suggested further simplifying the organic fraction into primary and secondary or aged contributions in favour of time and size resolution and testing this approach in further field experiments.

Online chemical analysis techniques for fine particulate matter have substantially advanced in recent years. With Aerodyne's Q-AMS (Jayne et al., 2000) an instrument delivering quantitative, highly time and size resolved chemical characterisation of the non-refractory fine particulate matter (NR-PM$_1$) has become commercially available. Aklilu et al. (2006) have combined chemical composition data from an Q-AMS with simplified model calculations applying the Zdanovskii-Stokes-Robinson (ZSR) mixing rule (Zdanovskii, 1948; Stokes and Robinson, 1966) and a constant organic growth

TORCH2 hygroscopicity closure

M. Gysel et al.

EGU

factor. Against the expectations expressed by McFiggans et al. (2005) they achieved reasonably good closure against HTDMA measurements when sulphate was the dominant inorganic compound, whereas in the presence of nitrate the predictions clearly overestimated the growth. Therefore they speculated that in their case the nitrate detected by the Q-AMS may have originated from organic nitrates instead of ammonium nitrate or that the ZSR mixing rule does not hold for particles containing ammonium nitrate.

In this study we applied a similar approach using Q-AMS data and ZSR modelling against HTDMA measurements within the second field experiment of the UK NERC-funded Tropospheric ORganic CHemistry project (TORCH2) in a location encountering predominantly aged air masses. We also found that closure is only achieved in the absence of significant nitrate loadings, but based on a larger data set covering a wider size range, we can state the hypothesis that the disagreement may be caused by an instrumental nitrate evaporation artefact.

2   Experimental and data analysis

2.1   Sampling site

Measurements were conducted in May 2004 at the Weybourne Atmospheric Observatory (WAO), which is located on the North Norfolk coastline near Weybourne, UK. Air masses encountered at this station represent aged polluted outflow from London, the West Midlands or the European continent for large scale wind directions south, west, or east, respectively, or relatively clean air masses transported across the North Sea region by northern wind. North Norfolk is a sparsely populated rural region without large population centres or industrial areas.

EGU

2.2 Instrumentation

Air was drawn down a 150 mm bore, 12 m high sampling stack at a flow rate of 150 l min^{-1}. The flow rate was such that diffusion losses for sub-micrometre particles were minimal above 5 nm diameter. Air was sub-sampled isokinetically from the main stack through a 40 mm bore stainless steel line, bending with a 1 m radius of curvature then running into the container, where a variety of instrumentation further sub-sampled from the 40 mm tube. The connections of HTDMA and Q-AMS were next to each other.

A HTDMA (Cubison et al., 2005) was used to measure hygroscopic growth factor distributions at 90% RH of particles with dry diameters D_0=27, 40, 60, 89, 137, and 217 nm. The hygroscopic growth factor of a particle is defined as $GF(\mathrm{RH})=D(\mathrm{RH})/D_0$, where $D(\mathrm{RH})$ is the diameter at a fixed RH. A detailed description of the instrument is given in Cubison et al. (2005). Briefly, the polydisperse ambient aerosol is first brought to charge equilibrium using a bipolar ^{90}Sr charger, before a monodisperse size cut is selected using a first Differential Mobility Analyser (DMA) operated with dried sheath air. These particles of known dry size are then conditioned to 90% RH, before passing through a cylindrical volume with a residence time of ~60 s. After that the size distribution of the grown particles is detected by scanning a second DMA operated at 90% RH across the relevant size range. Particles consisting of a single compound have a well defined growth factor at a fixed RH. Atmospheric aerosols typically contain several compounds which are externally or internally mixed in the different particles. Even in internally mixed aerosols it is to be expected that the relative fractions of compounds vary between individual particles. Therefore a range of growth factors or even clearly separated growth modes are often found, when measuring the "growth factor" of ambient particles of a defined dry size. Normalised growth factor probability distributions $c(GF)=dC/dGF$ are retrieved from each measurement, with total probability (C) of having a growth factor being unity ($C=\int c(GF)\,dGF=1$). The growth factor distributions were retrieved from the raw data using a method (Gysel et al., 2006[1]) with similarities

---

[1]Gysel, M., McFiggans, G. B., Coe, H., et al.: Inversion of TDMA data, in preparation, 2006.

EGU

to the OEM inversion algorithm described by Cubison et al. (2005). The distribution $c(GF)$ is also inverted from the measurement distribution into contributions from fixed classes of narrow growth factor ranges, but instead of using a linear inversion, $c(GF)$ is fitted to the actual measurements using a full TDMA transfer forward model. The advantage of this method is that application of the physical constraint $c(GF) \geq 0$ for all GF prevents propagation of oscillations in $c(GF)$ beyond the range of actual growth factors. Such oscillations occur when choosing too high resolution in GF.

The RH in the second DMA (RH_{DMA2}) generally reached the target of 90% within ±1% but for occasional larger drifts. In order to minimise effect of RH_{DMA2} drifts all growth factors measured between 88 and 90% RH were corrected to 90% RH using the following equation:

$$k(GF, a_w) = \frac{(GF^3 - 1)(1 - a_w)}{a_w} \iff GF(a_w, k) = \left(1 + k\frac{a_w}{1 - a_w}\right)^{\frac{1}{3}}, \tag{1}$$

where k captures all solute properties. First the k-value was calculated from the measured GF and RH (left hand side of Eq. 1), and then the corresponding corrected GF at 90% was calculated using this k (right hand side of Eq. 1). Eq. (1) is equivalent to Eq. (4) in the paper by Gysel et al. (2004) with $k = (M_w \cdot \rho_s \cdot i_s)/(\rho_w \cdot M_s)$, where M_w is the molar mass and ρ_w the density of water, and M_s the molar mass, ρ_s the density and i_s the van't Hoff factor of the solute. Equation (1) is also equivalent to Eq. (1) in the paper by Dick et al. (2000) with $a = k$ and $b = c = 0$, where $a, b,$ and c are their model parameters. More details about the theoretical background of the above functionality (Eq. 1) are given in Kreidenweis et al. (2005). Using a constant k-value for RH corrections is equivalent to a constant van't Hoff factor, which means constant deviation from ideal behaviour. This assumption is justified for small RH differences of only ±2% as chosen here.

Please note that Eq. (1) can also be used to extrapolate a growth factor given at a certain RH to a nearby RH under the assumption of constant k.

An Aerodyne quadrupole AMS (Q-AMS; Jayne et al., 2000) was used to provide

[EGU](#)

on-line, quantitative measurements of the chemical composition and mass size distributions of ambient NR-PM$_1$ at a high temporal resolution. The instrument works by sampling air through an aerodynamic lens to form a particle beam in a vacuum and accelerating the focussed beam of particles as a function of their momentum towards a tungsten heater (550°C) that flash vaporises the particles. The volatilisation stage is performed adjacent to an electron impact ioniser (70 eV) and the ions are analysed by a quadrupole mass spectrometer (QMA 410, Balzers, Liechtenstein) with unit mass-to-charge (m/z) resolution. In typical field operation, the Q-AMS alternates between two modes: (i) in the mass-spectrum (MS) mode the averaged chemical composition of the non-refractory aerosol ensemble is determined by scanning the m/z spectrum with the quadrupole mass spectrometer, without size resolved information, (ii) using the aerosol time-of-flight (ToF) mode the m/z of key chemical components can be resolved as a function of the vacuum aerodynamic diameter of the particles ($dM/d\log D_{va}$). More detailed descriptions of the Q-AMS measurement principles and various calibrations (Jayne et al., 2000; Canagaratna et al., 2006), its modes of operation (Jimenez et al., 2003) and data processing and analysis (Allan et al., 2003, 2004) are available in recent publications.

A dual Differential Mobility Particle Sizer (DMPS) system comprising a short and a long Vienna type DMA (Winkelmayr et al., 1991) in combination with a TSI 3025 and 3010 Condensation Particle Counter (CPC), respectively, was used to measure particle number size distributions from 4 to 827 nm. Total particle number concentrations were also measured with an additional CPC Model TSI 3025.

2.3 Hygroscopic growth predictions

Aerosol particles at RH<90% are concentrated solutions such that solute-solvent and solute-solute interactions influence the water activity of the solution. Semi-empirical models to predict growth factors of multicomponent inorganic/organic particles are available (Ming and Russell, 2002; Topping et al., 2005a,b). The Pitzer Simonson Clegg (PSC) mole fraction based approach (Clegg and Pitzer, 1992; Clegg et al., 1992)

TORCH2 hygroscopicity closure

M. Gysel et al.

Full Screen / Esc

Printer-friendly Version

Interactive Discussion

EGU

is generally used for inorganic mixtures, while the UNIFAC group contribution method (Fredenslund et al., 1975; Poling et al., 2001) is widely used for organic mixtures. However, mixed inorganic/organic solutions are not yet well characterised, and thus the models either ignore possible solute-solute interactions between inorganic and organic solutes (Topping et al., 2005b) or they introduce interaction parameters based on measurements of very few mixtures (Ming and Russell, 2002).

Solute-solute interactions are often small and can be neglected in good approximation (ZSR mixing rule; Zdanovskii, 1948; Stokes and Robinson, 1966), which is equivalent to

$$g_{\mathrm{mixed}}(a_w) \approx \left(\sum_i \varepsilon_i g_i(a_w)^3 \right)^{\frac{1}{3}} , \tag{2}$$

where a_w is the water activity, g_{mixed} is the growth factor of the mixed particle, g_i are the growth factors of the compounds in pure form, ε_i are the volume fractions of the compounds in the dry particle, and the summation goes over all compounds. Eq. (2) is the mixing rule for water activities thus g_{mixed} and g_i are the "flat surface equivalent" growth factors without Kelvin effect. For small droplets the Kelvin effect has to be taken into account, which is to be done as follows in a mathematically correct way: $g_{\mathrm{mixed}}(\mathrm{RH})$ can also be obtained with Eq. (2) but the water activity for all g_i's has to be chosen slightly smaller than RH such that $a_w \cdot S_k$=RH, where S_k is the Kelvin correction factor corresponding to the calculated droplet size $D(\mathrm{RH})=D_0 \cdot g_{\mathrm{mixed}}(RH)$. The solution can be found iteratively if the surface tension of the mixed solution is known. However, for the purpose of a hygroscopicity closure $g_{\mathrm{mixed}}(RH)$ can be obtained in good approximation by directly inserting the growth factors g_i at the same RH and D_0 into Eq. (2). The ZSR mixing rule in the form of Eq. (2) implicitly contains the assumption of volume additivity for the mixed particle droplet compared to the pure compound volumes. The ZSR relation (Eq. 2) shows that the growth factor of a mixed particle is at first driven by the relative abundance (expressed by ε_i) of more and less hygroscopic compounds, which is naturally to be expected. Furthermore the mixed particle growth factor is more

TORCH2 hygroscopicity closure

M. Gysel et al.

EGU

sensitive to uncertainties in growth factors of more hygroscopic compounds than of less hygroscopic compounds, which can be seen from the partial derivative by ∂g_i of Eq. (2):

$$\frac{\partial g_{\text{mixed}}}{\partial g_i} = \frac{\varepsilon_i g_i^2}{g_{\text{mixed}}^2}. \tag{3}$$

For a two compound particle with pure growth factors of $g_1 = 1.20$ and $g_2 = 1.80$, as an example, the critical volume fraction of compound 1 above which g_{mixed} is more sensitive to g_1 than to g_2 is as high as $g_1^2/(g_1^2 + g_2^2) = 0.69$. Therefore it is normally more important to know whether the growth factor of a more hygroscopic compound is 1.75 or 1.80 than whether the growth factor of a less hygroscopic compound is 1.15 or 1.20.

Models such as the ADDEM have not been used for the hygroscopicity closure in this study since the Q-AMS only provides an overall organic loading without speciation or detailed information on the organic composition in terms of functional groups and molecular size. Thus the growth model used here is reduced to the ZSR mixing rule (Eq. 2) applied for the major compounds measured by the Q-AMS: Ammonium sulphate ($(NH_4)_2SO_4$), ammonium bisulphate (NH_4HSO_4), sulphuric acid (H_2SO_4), ammonium nitrate (NH_4NO_3) and organics. If sulphuric acid was present, the growth factors calculated with Eq. (2) were corrected for the water associated with sulphuric acid at RH=5%. Growth factor values of all compounds are listed in Table 1. For the whole organic fraction a single "bulk" growth factor of $GF_{\text{org}} = 1.20$ at 90% RH was used. Taking the Kelvin effect with surface tension of pure water into account, this translates into an organic growth factor of 1.16, 1.18, and 1.19 for particles with dry diameter $D_0 = 60$, 137, and 217 respectively. This particular value for the "bulk" GF_{org} was chosen because it delivered best closure results. A discussion how this value compares with findings of earlier studies is provided in Sect. 4.

Volume fractions ε_i of inorganic salts and organic compounds are obtained from

respective mass fractions δ_k delivered by the Q-AMS via

$$\varepsilon_i = \frac{\frac{\delta_i}{\rho_i}}{\sum\limits_k \frac{\delta_k}{\rho_k}}, \tag{4}$$

where ρ_k denote the dry densities of the pure compounds. Volume additivity in the dry mixture is again assumed. Since only mass fractions and not absolute masses are needed in Eq. (4), the application of the ZSR mixing rule is independent of the collection efficiency of the Q-AMS for internally mixed particles and as long as no additional data such as EC from other chemical analysis techniques are used.

3 Results

3.1 Air mass origin

Meteorological parameters at the WAO (University of East Anglia) and five-day back trajectories (ECWMF) are shown in Figs. 1 and 2, respectively. The beginning of the measurement period (8–10 May) was characterised by frequent cloud cover, some rainfall and air masses (Fig. 2a) originating from continental Europe and transported across the north sea. From 11–13 May clean air masses originating from the Norwegian Sea or the Northeastern Atlantic Ocean were transported across the North Sea to the WAO without land contact for several days (Fig. 2b). During the period from 14–20 May there was dry and virtually cloud free weather with low wind speeds and air masses originating from the Northeastern Atlantic Ocean and transported across Ireland and North England or the English Midlands (Fig. 2c). However, during this period the local wind speed showed a diurnal pattern which is not captured by the back trajectories, most probably a sea breeze effect, with wind from the north during the day and wind from the south during the night. From 21–23 May again clean air masses from the Northeastern Atlantic Ocean were transported across the North Sea to the

EGU

site with possibly some land contact over northern Scotland (Fig. 2d). In the following the flow regimes described above will be referred to as "aged polluted 1" (8–10 May), "clean marine 1" (11–13 May), "aged polluted 2" (14–20 May), and "clean marine 2" (21–23 May).

3.2 Hygroscopic behaviour

Growth factor distributions $c(GF)$ (see above) along with the volumetric mean growth factor and the number fraction of particles with growth factor larger than 1.15 ($N_{GF>1.15}$) are shown in Fig. 3 with a time resolution of 1 h. Generally a strong influence of particle size and air mass type was observed. The events "clean marine 1" and "clean marine 2" were very similar, the growth factors at all dry sizes showed little variation over time and a single narrow growth mode indicating that the particles were nearly internally mixed with limited differences in composition between individual particles. As an exception around 10% of non-hygroscopic particles were observed at D_0=217 during the event "clean marine 2", which might be the remains of some short land contact over Scotland or from ship traffic in the north sea. It is worth noting that no externally mixed sea salt particles with growth factors larger than 2 have been found in the investigated size ranges. Similar behaviour but for slightly smaller growth factors was also observed during the event "aged polluted 1", where the air arrived from continental Europe across the North Sea. The event "aged polluted 2", influenced by more recent pollution over England, showed a clearly different picture: particles with dry sizes $D_0 \geq 89$ nm were externally mixed with a small fraction of non-hygroscopic particles ($GF \approx 1.0$) and a main mode of particles with growth factors varying between 1.3 and 1.6. The main growth mode, containing around 80 to 90% of the particles, was generally narrow though occasionally a clear spread of growth factors or even a third mode was seen. The mean growth factor of particles with $D_0 \leq 60$ nm, varied between 1.2 and 1.6, which is also the reason for the strong variations of $N_{GF>1.15}$ for small particles. Completely non-hygroscopic particles were not observed in this size range and there was no clearly detectable separation in two distinct modes, though there was

EGU

often a clear spread of growth factors in the main mode. This indicates that the small particles were not completely internally mixed with differences in composition between individual particles. The variations of growth factors and $N_{GF>1.15}$ showed a diurnal pattern strongly linked to the local wind direction with a minimum in mean growth factor and $N_{GF>1.15}$ after midnight and a maximum in mean growth factor and $N_{GF>1.15}$ after noon.

The RH-dependence of growth factors was also measured on four different days for both hydration and dehydration of particles (Fig. 5). "Hydration" means that the particles are exposed to increasing RH after dry selection in DMA1 with the maximum RH reached during wet size measurement in the second DMA (RH_{DMA2}, abscissa in Fig. 5). "Dehydration" means that the dry particles selected in DMA1 were exposed to RH>90% in a prehumidifier before conditioning to RH_{DMA2} <90% for wet size measurement. In praxis the hydration curve was first measured while reducing RH_{DMA2} from 90 down to ~10%, followed by the dehydration measurement while increasing RH_{DMA2} from ~10% back up to 90%. This order was chosen because the RH in DMA2 always lags somewhat behind the RH in the humidifier under transient conditions. Unfortunately the particle composition and thus hygroscopicity changed in some cases since a complete cycle lasted for 7–11 h. The emphasis was put on particle hydration in order to investigate the RH of water uptake onset and to see whether a pronounced deliquescence transition can be observed. On 21 May the particles showed gradually increasing growth factors with growth onset at RH as low as 40% RH without any indication of a deliquescence transition upon hydration. On 21 May the Q-AMS indicated an ammonia shortage, thus the presence of sulphuric acid and/or ammonium bisulphate is probably responsible that particles remain liquid at low RH and thus do not show a deliquescence clear deliquescence transition. No Q-AMS data is available for the humidogram on 9 May. A contrasting result was found on 14 and 19 May, where little or no growth was observed at RH<65%, followed by some growth in the range ~65–75% RH and a final deliquescence step at around 80% RH. On these two days the Q-AMS indicated that the sulphate was neutralised by ammonia, thus the deliques-

cence step at ~80% RH is attributed to ammonium sulphate. The growth in the range ~65–75% RH is probably due to organics and part of the sulphate, which starts to dissolve at lower RH in a mixed organic/ammonium sulphate particle (Marcolli et al., 2004; Marcolli and Krieger, 2006). Dehydration curves are also shown in Fig. 5, though they cannot be directly compared with the hydration curves for two reasons: on the one hand there is a time delay of a few hours between the two measurements, and on the other hand RH_{DMA2} was varied very rapidly for RH<75% resulting in large errors bars for dehydration curves. Nevertheless, the dehydration measurements still show that the particles remain dissolved down to at least 40% RH. Figure 5 also contains semi-empirical model curves calculated with Eq. (1, right hand side), where k was used as the only free model parameter to fit the curves to the measurements at RH>80%. For the humidograms in Fig. 5 the growth characteristics between 80 and 90% RH are well described by the above semi-empirical model with appropriate choices of k, indicating that the deviations from ideality of ambient particle solutions are nearly constant over a limited RH range. This also justifies the use of Eq. (1) to correct the measurements made within 88–92% RH to the target RH of 90% for the results shown in Fig. 3.

3.3 Particle number, mass and chemical composition

A CPC and a DMPS were used to measure the total particle number concentration and the particle number size distribution, respectively (D=4–827 nm). Figure 4a shows that the integrated number particle concentration from the DMPS size distribution agrees well with the direct measurement from the CPC. Panel a) also shows the integrated number of particles with diameters larger than 55 nm in order to provide a rough distinction between ultrafine and accumulation mode particles. The total particle number concentration varied massively from <500 to >20 000 cm^{-3}. Lowest number concentrations were observed during the two "clean marine" events, whereas highest number concentrations peaks observed during the "aged polluted 2" and "clean marine 1" events were most probably a result of recent nucleation events, as can be seen from the clear dominance of particles with diameters smaller than 55 nm.

EGU

The number size distributions have also been used to estimate the total fine aerosol mass by calculating the total integrated volume and multiplication by a density of 1600 kg m^{-3} (see below for discussion of particle density). In Fig. 4b the "DMPS-mass" is compared with the total NR-PM$_1$ detected by the Q-AMS, whereas the Q-AMS mass signal was multiplied by a factor of 2 in order to correct for an assumed collection efficiency of 0.5. The agreement between DMPS and Q-AMS mass is generally good, indicating that the instruments performed well. Exceptions, where the Q-AMS mass is distinctly higher (marked by orange circles in Fig. 4b), coincided with either very acidic aerosols or a high nitrate content, indicating that in these cases the Q-AMS collection efficiency might have been higher than 0.5 (Crosier et al., 2006[2]). Thus the reported Q-AMS data are probably over-corrected for collection efficiency in these events. The correlation also indicates that the refractory material such as elemental carbon, mineral dust and sodium chloride, which is not detected by the Q-AMS, is probably only a minor fraction. Please note that mass loadings reported here are only approximate, since the Q-AMS collection efficiency has not been quantified against other chemical analyses, but Q-AMS and DMPS data indicate total mass loadings in the order of 5–10, <5, 5–15, and <3 µg m^{-3} for the events "aged polluted 1", "clean marine 1", "aged polluted 2", and "clean marine 2", respectively.

The main Q-AMS data are SO$_4$, NO$_3$, NH$_4$ and organics, from which the inorganic salts have been derived by attribution of the measured NH$_4$ to NO$_3$ and SO$_4$. If less NH$_4$ was measured than needed to fully neutralise NO$_3$ and SO$_4$, then SO$_4$ was assumed to be present as (NH$_4$)$_2$SO$_4$ and NH$_4$HSO$_4$ or NH$_4$HSO$_4$ and H$_2$SO$_4$. Note, this choice of sulphate salts is crucial for correct application of the ZSR mixing rule, i.e. choosing a combination of H$_2$SO$_4$ and (NH$_4$)$_2$SO$_4$ to match the amounts of SO$_4$ and NH$_4$ would result in significant water uptake prediction errors. Splitting the sulphate salts based on the measured ammonium may not be highly accurate, particularly for the

---

[2]Crosier, J., Allan, J. D., Coe, H., Bower, K. N., Formenti, P., and Williams, P. I.: Chemical composition of summertime aerosol in the Po Valley (Italy), Northern Adriatic and Black Sea, Quart. J. Roy. Meteorol. Soc., submitted, 2006.

TORCH2 hygroscopicity closure

M. Gysel et al.

EGU

size resolved data, but it indicates at least whether the aerosol is neutralised or acidic. Again, the Q-AMS cannot measure refractory material such as elemental carbon, mineral dust and sodium chloride. Time and size dependent chemical composition from the Q-AMS is shown as relative contributions to the total detected mass (Fig. 6). Panel a) shows the integrated composition of the NR-PM$_1$ as measured in the MS-mode, while panels b) to d) show size resolved data obtained in the ToF-mode integrated over the size ranges 68–145, 145–309, and 309–659 nm vacuum aerodynamic diameter, respectively. These ranges correspond to centre mobility diameters of 66, 133, and 282 nm assuming spherical particles and a density of 1500, 1600, and 1600 kg m^{-3}, respectively. These density values are based on the mixed particle density according to the typical chemical composition observed in the respective size range. The densities the pure salts are well known and for the organic fraction a density of 1400 kg m^{-3} (Alfarra et al., 2006; Dinar et al., 2006) is assumed (Table 1). Unfortunately there are no reliable Q-AMS data for the "age polluted 1" event, due to technical faults with the Q-AMS electronics. Size resolved data below a critical minimum detected mass are also not shown. The two events "clean marine 1" and "clean marine 2" are characterised by ~80% of sulphates and ~20% organics, while there is no nitrate present nor is there a clear size dependence of the composition. The measurements also indicate an acidic aerosol, which is reasonable for trajectories without land contact for five days. During the "aged polluted 2" event there was, similar to the hygroscopic behaviour, a distinct diurnal pattern strongly linked with the local wind direction. Particularly sulphate and nitrate exhibited an opposite trend of maxima during daytime and nighttime, respectively. However, the total inorganic fraction remained fairly constant with around 60–80%, 40–60%, and 10–50%, in the (mobility) diameter bins 282, 133, and 66 nm respectively. Consequently also the organic fraction was fairly constant with around 20–40%, 40–60%, and 50–90% in the respective size bins.

The spectra of the organic mass fragments (not shown) resembled the spectra of aged organic aerosols found in other rural and remote locations (Alfarra et al., 2004; McFiggans et al., 2005) for typical mass spectra of various ambient organic aerosols).

EGU

The spectra during the two "clean marine" events had the "most remote" characteristics but also the spectra from the "aged polluted 2" event were clearly different from an urban aerosol. A diurnal pattern during the "aged polluted 2" event was also visible in the organic mass fragments but only as minor changes. A few key organic fragments in Q-AMS mass spectra provide basic information on the type of organic compounds present (Zhang et al., 2005a,b). The fragment m/z 57 $C_4H_9^+$ is a marker for hydrocarbons from primary emissions and has also been shown to correlate with EC in traffic dominated locations (Zhang et al., 2005a,b). m/z 43 can be either $C_3H_7^+$ from hydrocarbons or CH_3CO^+ from ketones, aldehydes or monocarboxylic acids. m/z 43 is thus a major fragment in both primary and secondary oxygenated organic aerosols, whereas the fragment m/z 44 (CO_2^+) from dicarboxylic or multifunctional organic acids) is a marker for secondary oxygenated organic acids. In Fig. 7a the contributions of the fragments m/z 43, 44 and 57 to the total organic mass loading are shown. m/z 44 is always equal or larger than m/z 43 and it contributes mostly around 10% to the total organics, occasionally even up to ∼20%. The contribution of m/z 57 is negligible during the "clean marine" events and up to ∼3% during the "aged polluted 2" event. These findings indicate dominance of highly oxidised organic compounds with some small contribution from primary hydrocarbons during the "aged polluted 2" event.

3.4 Hygroscopicity closure

In this study we try to achieve hygroscopicity closure for the investigated aerosol, which means reasonable agreement between measured and predicted hygroscopic growth factors. As described in Sect. 2.3 we used the ZSR relation to predict the mixed particle growth factor from pure compound behaviour and the chemical composition as measured by the Q-AMS. The Q-AMS provides the average composition of all particles of a given size without any information on the mixing state. Thus the HTDMA's growth factor distributions are averaged by volume in order to obtain a mean growth factor for comparison with the predicted values. Figure 8 shows the size resolved hygroscopicity closure with a time resolution of 2 h. The agreement between HTDMA

EGU

(red line) and AMS/ZSR prediction (blue line) is reasonably good during the two "clean marine" events, at sizes and times when sufficient signal is available. Good agreement is also found for 60-nm particles during the "aged polluted 2" event. However, during the latter event measured and predicted values for 137- and 217-nm particles disagree considerably and are rather anti-correlated than correlated.

An inappropriate choice of GF_{org} as a cause for the observed discrepancies can be ruled out as will be discussed below, but they could in principle arise from the fact that the Q-AMS cannot detect refractory material such as sodium chloride, sodium sulphate, mineral dust and elemental carbon. Sodium chloride and sodium sulphate are found in particles containing sea salt and they have "bulk" growth factors of 2.41 and 1.92 at 90% RH, respectively (ADDEM; Topping et al., 2005a). Thus not considering either of them in the ZSR model would lead to a strong underprediction of growth factors. It is unlikely that sodium chloride and sodium sulphate were present in significant amounts in the investigated size range since neither an underprediction of growth factor nor externally mixed particles with growth factors above 2 were observed in these cases where the air masses arrived across the North Sea. Both elemental carbon and mineral dust are not hygroscopic in pure form (Weingartner et al., 1997; Vlasenko et al., 2005), and not considering either of them in the ZSR model would indeed result in an overprediction of growth factors. Mineral dust is predominately found in coarse mode particles and there should not be major dust sources in the vicinity of the WAO. Thus we do not expect that mineral dust was present in significant amounts at investigated particle sizes. Elemental carbon on the other hand is predominately found in the fine aerosol fraction and small amounts are also found in aerosols at remote locations (Krivácsy et al., 2001). EC is thus a potential candidate for the discrepancies seen in Fig. 8. It was intended to use a volatility tandem DMA (VTDMA) to provide some information on the EC content of the particles but unfortunately this instrument failed. However, it will be discussed below that during this campaign the EC fraction was probably too small to have a major impact on measured growth factors and to explain the discrepancies.

TORCH2 hygroscopicity closure

M. Gysel et al.

Title Page

Abstract	Introduction
Conclusions	References
Tables	Figures

◄◄	►►
◄	►
Back	Close

Full Screen / Esc

Printer-friendly Version

Interactive Discussion

EGU

4   Discussion

The correlation between growth factors from AMS/ZSR prediction and from HTDMA measurement is shown in Fig. 9 on the left hand side panels. The colour code indicates the mass fraction of nitrate relative to the total mass detected by the Q-AMS in the re-
spective size ranges. While the points with low nitrate mass fractions (reddish colours) scatter about the 1:1-line, the points with high nitrate mass fractions (greenish colours) stand out with systematically overpredicted growth factors (or too low measurements). This finding is particularly well seen at D=137 and 217 nm, but also for the few points with high nitrate at D=60 nm. Based on this finding we made a modified AMS/ZSR
prediction by simply ignoring the NH_4NO_3. Strikingly, this modified AMS/ZSR prediction does a very good job for all sizes and times as can be seen from the centre panels in Fig. 9 and from the small difference between the red and blue lines in Fig. 10. The modified AMS/ZSR predictions correlate well with the measurement and there is good quantitative agreement, as can be seen from fitted slopes being very close to unity
for 137- and 217-nm particles (blue lines in Fig. 9). The modified AMS/ZSR prediction brings also the few points with high nitrate mass fraction at D=60 nm down to the 1:1-line. At this diameter the fitted slope drops from 0.95 for the original AMS/ZSR prediction to 0.84 for the modified prediction. However, the signal statistics in this size bin was sometimes at the lower limit, most probably leading to a couple of points with
overestimated organic mass fraction, since the Q-AMS's organic mass is the sum of many different m/z fragments with a very low signal to noise ratio.

The fact that such a simple "one-parameter" modification of the AMS/ZSR prediction is able to produce good agreement for all sizes and times is at first surprising but strongly suggests some systematic mechanism behind the presence of nitrate and
discrepancies in the hygroscopicity closure. As the AMS/ZSR predictions contain a number of assumptions and approximations, it has to be carefully checked, before drawing hasty conclusions, whether the discrepancies found with the basic closure (Fig. 8) and the good agreement found with the modified closure (Fig. 10) are not just

by chance the result of an inappropriate choice of tuneable parameters in the AMS/ZSR prediction. Possible reasons related to the presence of nitrate could be:

- – Matching the electrical mobility and vacuum aerodynamic mobility diameter fails when nitrate is present.

5
- – The approximation of volume additivity in the dry mixed particle is not fulfilled when nitrate is present.

- – The organic growth factor is smaller at times where nitrate is present.

- – The nitrates detected by the Q-AMS originate from organic nitrates with a significantly smaller growth factor than ammonium nitrate.

10
- – The presence of surface active compounds suppressing the water uptake correlates with nitrate.

- – The presence of EC correlates with nitrate.

- – The ZSR mixing rule does not apply if ammonium nitrate is present in the solution.

- – The discrepancies in the closure are not a result of prediction errors but rather
15   a measurement artefact in the HTDMA due to evaporation losses of NH_4NO_3 occurring before or in the HTDMA.

Particle density and shape factor are needed to match the electrical mobility diameter (DMA) and vacuum aerodynamic diameter (Q-AMS). The resulting effect on the composition at a certain mobility diameter is small, because the combined uncertainty of
20   shape factor and density is expected to be smaller than 20%. Pure compound density values also go into the calculation of volume fractions from mass fractions (Eq. 4), but the sensitivity is small. Strong deviations from volume additivity in the dry mixed particle can be ruled out as a cause for the deviations when nitrate is present, since the sensitivity of predicted growth factors is again too small. The growth factor of the

organic compounds may be different from the value chosen here ("bulk" GF_{org}=1.20 at 90% RH). Reducing GF_{org} to an expected minimum value of 1.0 at 90% RH (see green lines in Fig. 8), doesn't make much difference at larger sizes, since the mixed growth factor is insensitive to small changes in GF_{org} as discussed above. Reducing GF_{org} does on the other hand show an effect for 60-nm particles, where the organic fraction dominates. For the organic dominated 60-nm particles good agreement is obtained with $GF_{org}(60\,nm)$=1.16, which agrees with expectations for oxidised organics (see discussion below). Even though the organic growth factor can be used to vary the growth factor prediction at 60 nm a little, neither density nor GF_{org} assumptions can be used to fit the model predictions to the observed temporal variability.

The possibility that the detected nitrates originate mostly from organic nitrates instead of NH_4NO_3 is unlikely since the relative intensity of the fragments m/z 30 (NO^+) and m/z 46 (NO_2^+) in the mass spectrum is constantly ∼3, which is the characteristic value of NH_4NO_3. Possible effects of surface active compounds slowing down or suppressing the water uptake are a field of ongoing discussion (Chan and Chan, 2005; Johnson et al., 2005; McFiggans et al., 2006; Sjogren et al., 2006). However, so far there are no cast-iron measurements available that would indicate a significant effect at residence times of more than 60 s. Here one would have to assume a dramatic effect to achieve closure and thus we consider it to be an unlikely cause of observed discrepancies.

Alternatively to the modified prediction assuming complete NH_4NO_3 evaporation (Fig. 10), good closure can also be achieved by assuming the presence of inert EC proportional to the nitrate volume, i.e. V_{inert}=1.72·$V_{NH_4NO_3}$, in the AMS/ZSR prediction (not shown). Some link in the presence of nitrate and EC is possible since both originate from traffic emission, however, the factor 1.72 translates into an estimated EC mass fraction in the fine aerosol of up to ∼40%, which would be extremely high (Krivácsy et al., 2001; Putaud et al., 2004) for an aged aerosol according to the back trajectory analysis and thus cannot be expected. Furthermore, the organic fragment m/z 57, a marker for hydrocarbons from primary traffic emissions, has been shown to correlate

TORCH2 hygroscopicity closure

M. Gysel et al.

EGU

well with EC under strong influence from primary emissions by Zhang et al. (2005a,b). Their results roughly translate into an m/z 57 to EC mass ratio of ∼0.11. The above EC estimate would translate into an m/z 57 to EC mass ratio of ∼0.02. Based on these indices we believe that the virtual EC mass required to achieve closure is by far above a plausible value.

It can be seen from the growth factor distributions shown in Fig. 3 that a separated mode of non-hygroscopic particles is present during the "aged polluted 2" event, but their number fraction hardly exceeds 20%. These particles with a growth factor lower than 1.15 are likely to be soot particles composed of EC and primary organics. This is confirmed by the fact that the number fractions of non-hygroscopic particles at 217 and 137 nm correlate well with the mass fraction of the fragment m/z 57 in NR-PM$_1$ (Fig. 7b). Assuming 50–100% EC in the non-hygroscopic particles roughly translates into an m/z 57 to EC mass ratio of ∼0.05–0.1, which is in a reasonable range. Thus we have also calculated the mean growth factor of only those particles with $GF > 1.15$. The difference to the overall mean growth factor is small (see orange and red lines in Fig. 10), since the number fraction of non-hygroscopic particles is small. This is another indication that the EC content is too small to explain the discrepancies of the original closure.

Since the EC in the non-hygroscopic particles is not detected by the Q-AMS, one can argue, that the AMS/ZSR prediction should be compared with the mean growth factor of only the hygroscopic particles, even though the non-hygroscopic particles probably also contain organics on the one hand, and the hygroscopic particles may also contain some EC on the other hand. At most times the closure between the modified AMS/ZSR prediction and the hygroscopic mode only is indeed a little better than with the overall mean growth factor (Figs. 9 and 10).

Here we are back to the fact that the closure is only successful with the modified AMS/ZSR prediction, and there are only two possible reasons remaining from the above list: Either failure of the ZSR mixing rule or a measurement artefact in the HT-DMA when nitrate is present. A similar hygroscopicity closure has been done in a

EGU

recent study by Aklilu et al. (2006), where they found good agreement between measurement and AMS/ZSR prediction except for periods when nitrate was present. In the latter cases growth factors were overpredicted, which has been attributed to shortcomings of the ZSR relation in mixtures containing nitrate. The ZSR mixing rule takes non-ideal behaviour into account but for solute/solute interactions, which are typically small at high RH. Therefore ZSR predictions of water uptake agree within ±10% with the actual water uptake of the mixed electrolytes of atmospheric importance (Topping et al., 2005a), which translates into GF prediction errors of <3%, provided that the sulphate salts representing SO_4 and NH_4 are correctly chosen (see Sect. 3.3). Marcolli and Krieger (2006) have shown for a range of organics mixed with NaCl, $(NH_4)_2SO_4$ or NH_4NO_3 that the electrolyte/organic interactions do influence the organic and salt solubility but hardly have an influence on the water activity, i.e. that the ZSR rule can be applied with small errors. In this study only a reduction of the pure NH_4NO_3 growth factor by as much as 27% in the AMS/ZSR prediction would be enough to achieve good closure with measurements. If true, this would be a very strong violation of the ZSR mixing rule and thus we much rather believe that an evaporation artefact in the HTDMA is the reason for failure of closure in the presence of nitrate.

Particulate NH_4NO_3 is well known to cause negative (evaporation) or positive (sorption) sampling artefacts in various aerosol sampling techniques. Evaporation losses of NH_4NO_3 can occur if either the gas phase vapour pressure product of ammonia and nitric acid is decreased or if the equilibrium vapour pressure product is increased due to changes in temperature or particle composition. The equilibrium vapour pressure product of gaseous ammonia and nitric acid over aqueous solutions increases with temperature and increases with decreasing RH (Dassios and Pandis, 1999), while over solid NH_4NO_3 it appears to increase with increasing RH (Mikhailov et al., 2004). Mixed $(NH_4)_2SO_4/NH_4NO_3$ aqueous solutions decrease the equilibrium vapour pressure substantially (Seinfeld and Pandis, 1998). Dassios and Pandis (1999) have used a TDMA set up with a laminar flow evaporation cell to measure evaporation rates of pure NH_4NO_3 particles. They have reported evaporation times of ~30 s for 100-nm

TORCH2 hygroscopicity closure

M. Gysel et al.

EGU

TORCH2 hygroscopicity closure

M. Gysel et al.

particles at room temperature and 10% RH. Mikhailov et al. (2004) have also observed evaporation losses for pure NH_4NO_3 particles of up to 27 vol% during a residence time of ~11 s depending on RH. In this study the aerosol experienced first changes in the sampling line, where it was heated up from ambient temperature (~10–18°C) to laboratory temperature (24–26°C), also resulting in a decrease of RH from ~60–90% down to ~40% (see Fig. 1). Thus a fraction of NH_4NO_3 may have been lost in the inlet system, but obviously not completely according to the Q-AMS measurements. In the Q-AMS instrument itself the residence time before the flash vaporiser is only ~5 ms and the aerosol is exposed to a supersonic expansion accompanied by rapid cooling, which freezes the nitrate onto the particles. In the HTDMA the particles are exposed to RH<10% when entering DMA1, resulting in an increase of the equilibrium vapour pressure. Gaseous nitric acid is most probably depleted in the DMA's sheath air, since it is expected to be lost in the tubing and Nafion dryer. Therefore NH_4NO_3 is likely to evaporate in the HTDMA to some extent. The evaporation losses may either occur at the very beginning of DMA1, in which case the particles are measured as if no NH_4NO_3 was present at all, or in between DMA1 and DMA2 (~60 s), in which case the evaporative shrinking and hygroscopic growth are overlaid. Good closure (Figs. 9 and 10) can be achieved, if all NH_4NO_3 is assumed to evaporate at the very beginning of DMA1, or alternatively if ~61% of NH_4NO_3 are assumed to be lost between DMA1 and DMA2, corresponding to the alternative growth factor reduction of NH_4NO_3 by 27% as mentioned above. We strongly believe that the HTDMA measurements are biased by evaporation losses of NH_4NO_3 and, based on the evaporation time scales given in Dassios and Pandis (1999) and Mikhailov et al. (2004), we rather favour the second alternative. Evaporation losses of NH_4NO_3 may occur in any HTDMA with residence times larger than a few seconds. Also Aklilu et al. (2006) found in their study overprediction of growth factors when nitrate was present, and there was no positive correlation between nitrate and measured growth factors. These findings fit well into the picture of evaporative nitrate losses in the HTDMA. Thus it would be desirable to see whether simply ignoring NH_4NO_3 in their AMS/ZSR prediction would also be the

remedy to solve the discrepancies in their closure.

A further implication of the above findings is that any HTDMA measurements of ambient particles might suffer from an ammonium nitrate artefact if not otherwise proven. As a consequence growth factors measured by a HTDMA might be considerably smaller
5   than what they would be for undisturbed ambient particles as suggested by the closure results shown in Fig. 8.

The fractional contribution of the major compounds to the particle's water uptake according to the original AMS/ZSR prediction is shown in Fig. 11. The inorganic compounds completely dominate the water uptake at 137 and 217 nm with more than 90
10 and 80% fractional contribution, respectively. In periods with higher organic to sulphate mass ratios the inorganic mass fraction is kept high by the presence of NH_4NO_3. Thus the organic contribution in this size range is always very minor. At 60 nm, where the organic mass fraction is ~50–90%, the fractional contribution of the organics to the water uptake reaches ~20–50%. Sulphate vastly dominated the water uptake during
15 the "clean marine" events, while NH_4NO_3 was comparably important during the "aged polluted" events. The above numbers refer to the closure according to the aerosol composition measured by the Q-AMS.

The degree of neutralisation of sulphate by ammonium has been taken into account in both the original and modified AMS/ZSR prediction presented here. Additional cal-
20 culations with the assumption of full neutralisation of sulphate have also been made. The result (not shown) was an underprediction of growth factors during the periods when the aerosol was acidic. This finding confirms that it is important to take the neutralisation state of sulphate into account, since the ZSR mixing rule is most sensitive to the growth factors of the most hygroscopic compounds involved, as discussed above
25 in Sect. 2.3.

Best results in the above hygroscopicity closure for the aged aerosol encountered during TORCH2 were obtained with a "bulk" organic growth factor of GF_{org}=1.2 at 90% RH (see Table 1 for corresponding growth factors at small particle sizes). It is not possible to use the closure to derive GF_{org} precisely, but the closure results show that

EGU

GF_{org} is likely to be larger than 1.1 and smaller than 1.3. Aklilu et al. (2006) inferred, from a hygroscopicity closure on ambient aerosol at two different sites, organic growth factors at 80% RH of 1.03–1.04 and 1.11–1.14 during periods influenced by urban emission and dominated by secondary particulate matter, respectively. These values roughly correspond to 1.07–1.09 and 1.22–1.28 at 90% when using Eq. (1) to correct for the RH difference. Carrico et al. (2005) have shown that the growth factor of the organics in carbonaceous matter dominated and biomass burning influenced aerosol in the Yosemite National Park is in the order of 1.11–1.16 at 80% RH, which corresponds (Eq. 1) to about 1.22–1.30 at 90% RH. Hygroscopic growth factors at 90% RH of humic-like substances isolated from ambient filter samples have been reported to be ~1.18 (Gysel et al., 2004). McFiggans et al. (2005) have calculated a growth factor of ~1.11 at 90% RH for organic model compounds according to H-NMR functional group analysis of organics from ambient filter samples. Secondary organic aerosol formed by photooxidation of volatile organic precursors in smog chamber experiments has been found to have a growth factor of ~1.11 at 85% RH, which corresponds to about 1.17 at 90% RH (Baltensperger et al., 2005). Multifunctional organic acids have been shown to have growth factors of ~1.46 (Peng et al., 2001), whereas e.g. fatty acids and alkanes have growth factors of 1.0 at 90% RH due to insufficient solubility, though neither of the latter two compounds classes is expected to dominate the organics in aged atmospheric aerosol. A "bulk" growth factor in the order of GF_{org}=1.2 at 90% RH as inferred for the TORCH2 aerosol is in good agreement with the results of the above studies.

5 Conclusions and outlook

Chemical composition and hygroscopic growth factors of aerosol particles in air masses covering a range from very little to moderate aged anthropogenic influence have been investigated during the TORCH2 field experiment. Both particle composition and hygroscopicity were seen to be highly variable in time and strongly dependent on particle size. The ZSR mixing rule was used to predict particle hygroscopic growth

Title Page

Abstract | Introduction

Conclusions | References

Tables | Figures

◄◄ | ►►

◄ | ►

Back | Close

Full Screen / Esc

Printer-friendly Version

Interactive Discussion

EGU

factors from their composition as measured by the Q-AMS. The major outcomes of the closure between predicted and measured growth factors are:

- Chemical composition data must be acquired with high resolution in both time and particle size. The Aerodyne Q-AMS is a suitable instrument as long as the aerosol is dominated by non-refractory (detectable) compounds. In aerosols containing substantial amounts of EC, mineral dust or sea salt, these compounds must also be measured with high resolution in both time and particle size. However, this may turn out to be difficult as better size resolution typically can only be achieved at lower time resolution, and different measurement techniques must agree quantitatively.

- Good closure was achieved in the absence of nitrate, but it completely failed in the presence of nitrate. This finding strongly suggests a systematic problem when nitrate is present. The authors of an earlier study (Aklilu et al., 2006) attributed a similar finding to shortcomings of the ZSR relation for mixtures containing NH_4NO_3. Based on the results from this study we rather believe that an NH_4NO_3 evaporation artefact in the HTDMA is the reason for the discrepancies.

- Quantitative closure could be achieved with the assumption of either a complete loss of NH_4NO_3 upon entrance in DMA1 or alternative ~60% loss during residence between DMA1 and DMA2 of the HTDMA. These results strongly indicate on the one hand that growth factors of ambient particles can be predicted from chemical composition by application of the ZSR relation within experimental uncertainty, and on the other hand that there is an artefact in the HTDMA measurements of ambient particles due to evaporation losses of NH_4NO_3.

- The closure shows that the mean "bulk" growth factor of organic compounds in the aged atmospheric aerosol particles encountered during TORCH2 is in the order of GF_{org}=1.2 at 90% RH. Thus the organic contribution to water uptake is minor (<20% at D >137 nm), except for small (D=60 nm) organic-dominated particles.

TORCH2 hygroscopicity closure

M. Gysel et al.

◀◀ | ▶▶

◀ | ▶

Back | Close

Full Screen / Esc

Printer-friendly Version

Interactive Discussion

EGU

– The inorganic fraction dominates the hygroscopic water uptake at high RH with a fractional contribution of more than 80% at $D{>}137$ nm. Sulphate dominated during "clean" events, while NH_4NO_3 became comparably important during the "aged polluted" events.

– It is more important to know the exact inorganic composition well (e.g. ammonium nitrate mass fraction and sulphate acidity), than to know the growth factor of the organic compounds accurately, because predictions of hygroscopic growth factors are more sensitive to the growth factors of the most hygroscopic compounds, whereas the sensitivity to growth factors of non- or moderately hygroscopic compounds is small. The exact organic GF becomes only important for organic volume fractions larger than ~70%.

Based on the closure results it has been hypothesised that the HTDMA measurements suffered from an artefact due to evaporation of NH_4NO_3, with the following implications:

– Hygroscopic growth factors of ambient particles measured by a HTDMA might be considerably underestimated if NH_4NO_3 is present, which is often a major compound in aged polluted air masses.

– Measurements of the composition of ambient aerosol particles up and downstream of an HTDMA should be made in order to reject or quantify evaporation artefacts.

– Instrument modifications and measurement strategies should be developed to minimise the artefact, if it should be proven to occur.

– Similar artefacts may occur during any HTDMA measurement of particles containing volatile compounds in equilibrium with the gas phase. Efforts to assure full equilibration of growth factors by application of longer residence times might increase evaporation artefacts.

TORCH2 hygroscopicity closure

M. Gysel et al.

Printer-friendly Version

Interactive Discussion

EGU

– In the presence of NH_4NO_3 model predictions of hygroscopic growth factors might be more representative of the undisturbed atmospheric aerosol than values measured with a HTDMA. However, chemical measurements are also very sensitive to NH_4NO_3 artefacts, but as long as they are not positive, the improvement of the model over the measurement goes into the right direction.

The hygroscopicity closure presented here has been made for the "bulk" composition in narrow size cuts as no single particle composition is obtained with the Aerodyne Q-AMS. The HTDMA data show that the particles are often not fully internally mixed. A next step in closure studies would be to predict the full growth distribution, which is only possible if quantitative single particle composition can be measured including the relative abundance of different particle types.

References

Aklilu, Y., Mozurkewich, M., Prenni, A. J., Kreidenweis, S. M., Alfarra, M. R., Allan, J. D., Anlauf, K., Brook, J., Leaitch, W. R., Sharma, S., Boudries, H., and Worsnop, D. R.: Hygroscopicity of particles at two rural, urban influenced sites during Pacific 2001: Comparison with estimates of water uptake from particle composition, Atmos. Env., 40, 2650–2661, 2006. 12506, 12525, 12526, 12528, 12529

Alfarra, M. R., Coe, H., Allan, J. D., Bower, K. N., Boudries, H., Canagaratna, M. R., Jimenez, J. L., Jayne, J. T., Garforth, A. A., Li, S. M., and Worsnop, D. R.: Characterization of urban and rural organic particulate in the lower Fraser valley using two aerodyne aerosol mass spectrometers, Atmos. Env., 38, 5745–5758, 2004. 12518

Alfarra, M. R., Paulsen, D., Gysel, M., Garforth, A. A., Dommen, J., Prévôt, A. S. H., Worsnop, D. R., Baltensperger, U., and Coe, H.: A mass spectrometric study of secondary organic

[EGU](#)

aerosols formed from the photooxidation of anthropogenic and biogenic precursors in a re-action chamber, Atmos. Chem. Phys., 6, 5279–5293, 2006, http://www.atmos-chem-phys.net/6/5279/2006/. 12518, 12537

Allan, J. D., Jimenez, J. L., Williams, P. I., Alfarra, M. R., Bower, K. N., Jayne, J. T., Coe, H., and Worsnop, D. R.: Quantitative sampling using an Aerodyne aerosol mass spectrom-eter 1. Techniques of data interpretation and error analysis, J. Geophys. Res, 108, 4090, doi:10.1029/2002JD002 358, 2003. 12510

Allan, J. D., Bower, K. N., Coe, H., Boudries, H., Jayne, J. T., Canagaratna, M. R., Millet, D. B., Goldstein, A. H., Quinn, P. K., Weber, R. J., and Worsnop, D. R.: Submicron aerosol composition at Trinidad Head, California, during ITCT 2K2: Its relationship with gas phase volatile organic carbon and assessment of instrument performance, J. Geophys. Res, 109, 2004. 12510

Baltensperger, U., Kalberer, M., Dommen, J., Paulsen, D., Alfarra, M. R., Coe, H., Fisseha, R., Gascho, A., Gysel, M., Nyeki, S., Sax, M., Steinbacher, M., Prevot, A. S. H., Sjögren, S., Weingartner, E., and Zenobi, R.: Secondary organic aerosols from anthropogenic and biogenic precursors, Faraday Discuss., 130, 265–278, 2005. 12528

Berg, O. H., Swietlicki, E., Frank, G., Martinsson, B. G., Cederfelt, S. I., Laj, P., Ricci, L., Berner, A., Dusek, U., Galambos, Z., Mesfin, N., Yuskiewicz, B., Wiedensohler, A., Stratmann, F., and Orsini, D.: Comparison of observed and modeled hygroscopic behavior of atmospheric particles, Contr. Atmos. Phys., 71, 47–64, 1998. 12506

Canagaratna, M. R., Jayne, J. T., Jimenez, J. L., Allan, J. D., Alfarra, M. R., Zhang, Q., Onasch, T. B., Drewnick, F., Coe, H., Middlebrook, A., Delia, A., Williams, L. R., Trimborn, A. M., Northway, M. J., Kolb, C. E., Davidovits, P., and Worsnop, D. R.: Chemical and microphysical characterization of ambient aerosols with the Aerodyne aerosol mass spectrometer, Mass Spec. Rev., in press, 2006. 12510

Carrico, C. M., Kreidenweis, S. M., Malm, W. C., Day, D. E., Lee, T., Carrillo, J., McMeeking, G. R., and Collett Jr., J. L.: Hygroscopic growth behavior of a carbon-dominated aerosol in Yosemite National Park, Atmos. Env., 39, 1393–1404, 2005. 12528

Chan, M. N. and Chan, C. K.: Mass transfer effects in hygroscopic measurements of aerosol particles, Atmos. Chem. Phys., 5, 2703–2712, 2005, http://www.atmos-chem-phys.net/5/2703/2005/. 12523

Clegg, S. L. and Pitzer, K. S.: Thermodynamics of multicomponent, miscible, ionic-solutions: generalized equations for symmetrical electrolytes, J. Phys. Chem., 96, 3513–3520, 1992.

TORCH2 hygroscopicity closure

M. Gysel et al.

Title Page

Abstract	Introduction
Conclusions	References
Tables	Figures

⏮ ⏭

◀ ▶

Back | Close

Full Screen / Esc

Printer-friendly Version

Interactive Discussion

EGU

12510

Clegg, S. L., Pitzer, K. S., and Brimblecombe, P.: Thermodynamics of multicomponent, miscible, ionic solutions. 2. Mixtures including unsymmetrical electrolytes, J. Phys. Chem., 96, 9470–9479, 1992. 12510

5 Cubison, M., Coe, H., and Gysel, M.: Retrieval of hygroscopic tandem DMA measurements using an optimal estimation method., J. Aerosol Sci., 36, 846–865, 2005. 12508, 12509

Dassios, K. G. and Pandis, S. N.: The mass accommodation coefficient of ammonium nitrate aerosol, Atmos. Env., 33, 2993–3003, 1999. 12525, 12526

Dick, W. D., Saxena, P., and McMurry, P. H.: Estimation of water uptake by organic compounds
10 in submicron aerosols measured during the Southeastern Aerosol and Visibility Study, J. Geophys. Res, 105, 1471–1479, 2000. 12506, 12509

Dinar, E., Mentel, T. F., and Rudich, Y.: The density of humic acids and humic like substances (HULIS) from fresh and aged wood burning and pollution aerosol particles, Atmos. Chem. Phys., 6, 5213–5224, 2006,
15 http://www.atmos-chem-phys.net/6/5213/2006/. 12518, 12537

Fredenslund, A., Jones, R. L., and Prausnitz, J. M.: Group-contribution estimation of activity-coefficients in nonideal liquid-mixtures, Aiche J., 21, 1086–1099, 1975. 12511

Gysel, M., Weingartner, E., and Baltensperger, U.: Hygroscopicity of aerosol particles at low temperatures. 2. Theoretical and experimental hygroscopic properties of laboratory gener-
20 ated aerosols, Env. Sci. Tech., 36, 63–68, 2002. 12505

Gysel, M., Nyeki, S., Paulsen, D., Weingartner, E., Baltensperger, U., Galambos, I., and Kiss, G.: Hygroscopic properties of water-soluble matter and humic-like organics in atmospheric fine aerosol, Atmos. Chem. Phys., 4, 35–50, 2004,
http://www.atmos-chem-phys.net/4/35/2004/. 12506, 12509, 12528

25 Hämeri, K., Charlson, R., and Hansson, H. C.: Hygroscopic properties of mixed ammonium sulfate and carboxylic acids particles, Aiche J., 48, 1309–1316, 2002. 12505

Hand, J. L., Kreidenweis, S. M., Sherman, D. E., Collett, J. L., Hering, S. V., Day, D. E., and Malm, W. C.: Aerosol size distributions and visibility estimates during the Big Bend regional aerosol and visibility observational (BRAVO) study, Atmos. Env., 36, 5043–5055,
30 2002. 12505

Jayne, J. T., Leard, D. C., Zhang, X. F., Davidovits, P., Smith, K. A., Kolb, C. E., and Worsnop, D. R.: Development of an aerosol mass spectrometer for size and composition analysis of submicron particles, Aerosol Sci. Tech., 33, 49–70, 2000. 12506, 12509, 12510

TORCH2 hygroscopicity closure

M. Gysel et al.

EGU

Jimenez, J. L., Jayne, J. T., Shi, Q., Kolb, C. E., Worsnop, D. R., Yourshaw, I., Seinfeld, J. H., Flagan, R. C., Zhang, X. F., Smith, K. A., Morris, J. W., and Davidovits, P.: Ambient aerosol sampling using the Aerodyne Aerosol Mass Spectrometer, J. Geophys. Res., 108, 8425, doi:10.1029/2001JD001213, 2003. 12510

Johnson, G. R., Ristovski, Z. D., D'Anna, B., and Morawska, L.: Hygroscopic behavior of partially volatilized coastal marine aerosols using the volatilization and humidification tandem differential mobility analyzer technique, J. Geophys. Res., 110, D20203, doi:10.1029/2004JD005657, 2005. 12523

Kay, M. J. and Box, M.: Radiative effects of absorbing aerosols and the impact of water vapor, J. Geophys. Res, 105, 12 221–12 234, 2000. 12505

Kreidenweis, S. M., Koehler, K., DeMott, P. J., Prenni, A. J., Carrico, C., and Ervens, B.: Water activity and activation diameters from hygroscopicity data – Part I: Theory and application to inorganic salts, Atmos. Chem. Phys., 5, 1357–1370, 2005, http://www.atmos-chem-phys.net/5/1357/2005/. 12509

Krivácsy, Z., Hoffer, A., Sárvári, Z., Temesi, D., Baltensperger, U., Nyeki, S., Weingartner, E., Kleefeld, S., and Jennings, S. G.: Role of organic and black carbon in the chemical composition of atmospheric aerosol at European background sites, Atmos. Env., 35, 6231–6244, 2001. 12520, 12523

Marcolli, C. and Krieger, U. K.: Phase changes during hygroscopic cycles of mixed organic/inorganic model systems of tropospheric aerosols, J. Phys. Chem., A110, 1881–1893, 2006. 12516, 12525

Marcolli, C., Luo, B., and Peter, T.: Mixing of the organic aerosol fractions: liquids as the thermodynamically stable phases, J. Phys. Chem., A108, 2216–2224, 2004. 12516

McFiggans, G., Alfarra, M. R., Allan, J., Bower, K., Coe, H., Cubison, M., Topping, D., Williams, P., Decesari, S., Facchini, C., and Fuzzi, S.: Simplification of the representation of the organic component of atmospheric particulates, Faraday Discuss., 130, 341–362, 2005. 12506, 12507, 12518, 12528

McFiggans, G., Artaxo, P., Baltensperger, U., Coe, H., Facchini, M., Feingold, G., Fuzzi, S., Gysel, M., Laaksonen, A., Lohmann, U., Mentel, T., Murphy, D., O'Dowd, C., Snider, J., and Weingartner, E.: The effect of physical and chemical aerosol properties on warm cloud droplet activation, Atmos. Chem. Phys., 6, 2593–2649, 2006, http://www.atmos-chem-phys.net/6/2593/2006/. 12523

Mikhailov, E., Vlasenko, S., Niessner, R., and Pöschl, U.: Interaction of aerosol particles com-

Title Page

Abstract | Introduction

Conclusions | References

Tables | Figures

|◄ | ►|

◄ | ►

Back | Close

Full Screen / Esc

Printer-friendly Version

Interactive Discussion

EGU

posed of protein and salts with water vapor: hygroscopic growth and microstructural rearrangement, Atmos. Chem. Phys., 4, 323–350, 2004, http://www.atmos-chem-phys.net/4/323/2004/. 12525, 12526

Ming, Y. and Russell, L. M.: Thermodynamic equilibrium of organic-electrolyte mixtures in aerosol particles, Aiche J., 48, 1331–1348, 2002. 12510, 12511

Peng, C., Chan, M. N., and Chan, C. K.: The hygroscopic properties of dicarboxylic and multifunctional acids: Measurements and UNIFAC predictions, Env. Sci. Tech., 35, 4495–4501, 2001. 12528

Poling, B. E., Prausnitz, J. M., and O'Connell, J. P.: The Properties of Gases and Liquids, McGraw-Hill, New York, 5 edn., 2001. 12511

Putaud, J. P., Raes, F., Van Dingenen, R., Brüggemann, E., Facchini, M. C., Decesari, S., Fuzzi, S., Gehrig, R., Hüglin, C., Laj, P., Lorbeer, G., Maenhaut, W., Mihalopoulos, N., Mülller, K., Querol, X., Rodriguez, S., Schneider, J., Spindler, G., ten Brink, H., Trseth, K., and Wiedensohler, A.: European aerosol phenomenology-2: chemical characteristics of particulate matter at kerbside, urban, rural and background sites in Europe, Atmos. Env., 38, 2579–2595, 2004. 12523

Ramanathan, V., Crutzen, P. J., Kiehl, J. T., and Rosenfeld, D.: Aerosols, climate, and the hydrological cycle, Science, 294, 2119–2124, 2001. 12505

Saxena, P., Hildemann, L. M., McMurry, P. H., and Seinfeld, J. H.: Organics alter hygroscopic behavior of atmospheric particles, J. Geophys. Res., 100, 18 755–18 770, 1995. 12506

Seinfeld, J. H. and Pandis, S. N.: Atmospheric Chemistry and Physics. From Air Pollution to Climate Change, John Wiley & Sons, Inc., New York, pp. 531 ff., 1998. 12525

Sjogren, S., Gysel, M., Weingartner, E., Baltensperger, U., Cubison, M., Coe, H., Zardini, A., Marcolli, C., Krieger, U., and Peter, T.: Hygroscopic growth and water uptake kinetics of two-phase aerosol particles consisting of ammonium sulfate, adipic and humic acid mixtures, J. Aerosol Sci., accepted, 2006. 12523

Stokes, R. H. and Robinson, R. A.: Interactions in aqueous nonelectrolyte solutions. I. Solute-solvent equilibria, J. Phys. Chem., 70, 2126–2130, 1966. 12506, 12511

Swietlicki, E., Zhou, J. C., Berg, O. H., Martinsson, B. G., Frank, G., Cederfelt, S. I., Dusek, U., Berner, A., Birmili, W., Wiedensohler, A., Yuskiewicz, B., and Bower, K. N.: A closure study of sub-micrometer aerosol particle hygroscopic behaviour, Atmos. Res., 50, 205–240, 1999. 12506

Topping, D. O., McFiggans, G. B., and Coe, H.: A curved multi-component aerosol hygroscop-

icity model framework: Part 1 - Inorganic compounds, Atmos. Chem. Phys., 5, 1205–1222, 2005a. 12505, 12510, 12520, 12525, 12537

Topping, D. O., McFiggans, G. B., and Coe, H.: A curved multi-component aerosol hygroscopicity model framework: Part 2 – Including organic compounds, Atmos. Chem. Phys., 5, 1223–1242, 2005b. 12505, 12510, 12511

Vlasenko, A., Sjögren, S., Weingartner, E., Gäggeler, H. W., and Ammann, M.: Generation of submicron Arizona test dust aerosol: Chemical and hygroscopic properties, Aerosol Sci. Tech., 39, 452–460, 2005. 12505, 12520

Weingartner, E., Burtscher, H., and Baltensperger, U.: Hygroscopic properties of carbon and diesel soot particles, Atmos. Env., 31, 2311–2327, 1997. 12505, 12520

Weingartner, E., Sjögren, S., Cozic, J., Verheggen, B., Baltensperger, U., Alfarra, M. R., Bower, K. N., Flynn, M. J., Gysel, M., and Coe, H.: Hygroscopic properties and chemical composition of aerosol particles at the high alpine site Jungfraujoch, J. Aerosol Sci., 35, S135–S136, 2004. 12506

Winkelmayr, W., Reischl, G. P., Lindner, A. O., and Berner, A.: A new electromobility spectrometer for the measurement of aerosol size distributions in the size range from 1 to 1000 nm, J. Aerosol Sci., 22, 289–296, 1991. 12510

Wise, M. E., Surratt, J. D., Curtis, D. B., Shilling, J. E., and Tolbert, M. A.: Hygroscopic growth of ammonium sulfate/dicarboxylic acids, J. Geophys. Res., 108, 4638, doi:10.1029/2003JD003775, 2003. 12505

Zdanovskii, A.: New methods for calculating solubilities of electrolytes in multicomponent systems, Zhur. Fiz. Khim., 22, 1475–1485, 1948. 12506, 12511

Zhang, Q., Alfarra, M. R., Worsnop, D. R., Allan, J. D., Coe, H., Canagaratna, M. R., and Jimenez, J. L.: Deconvolution and quantification of hydrocarbon-like and oxygenated organic aerosols based on aerosol mass spectrometry, Env. Sci. Tech., 39, 4938–4952, 2005a. 12519, 12524

Zhang, Q., Worsnop, D. R., Canagaratna, M. R., and Jimenez, J. L.: Hydrocarbon-like and oxygenated organic aerosols in Pittsburgh: insights into sources and processes of organic aerosols, Atmos. Chem. Phys., 5, 3289–3311, 2005b. 12519, 12524

TORCH2 hygroscopicity closure

M. Gysel et al.

EGU

Table 1. Density and growth factors of all compounds used in the hygroscopicity closure (Topping et al., 2005a).

	Density ρ [kg m^{-3}]	GF(90%) D_0=60 nm [-]	GF(90%) D_0=137 nm [-]	GF(90%) D_0=217 nm [-]	GF(90%) D_0=∞ [-]
$(NH_4)_2SO_4$	1769	1.66	1.70	1.72	1.73
NH_4HSO_4	1780	1.74	1.78	1.80	1.81
H_2SO_4	1830	2.02[a]	2.05[a]	2.06[a]	2.07[a]
NH_4NO_3	1720	1.74	1.80	1.82	1.83
Organics	1400[b]	1.16[c]	1.18[c]	1.19[c]	1.20[c]

[a] Sulphuric acid is expected to retain water at 5–10% RH corresponding to a growth factor of ~1.15, which is taken into account when calculating the mixed particle growth factor at 90% RH.
[b] The density of organics was chosen to represent oxidised organics in aged atmospheric aerosol (Alfarra et al., 2006; Dinar et al., 2006).
[c] The "bulk" organic growth factor was fitted for best hygroscopicity closure results. The corresponding growth factors for given D_0 were calculated from the "bulk" value assuming surface tension of pure water.

EGU
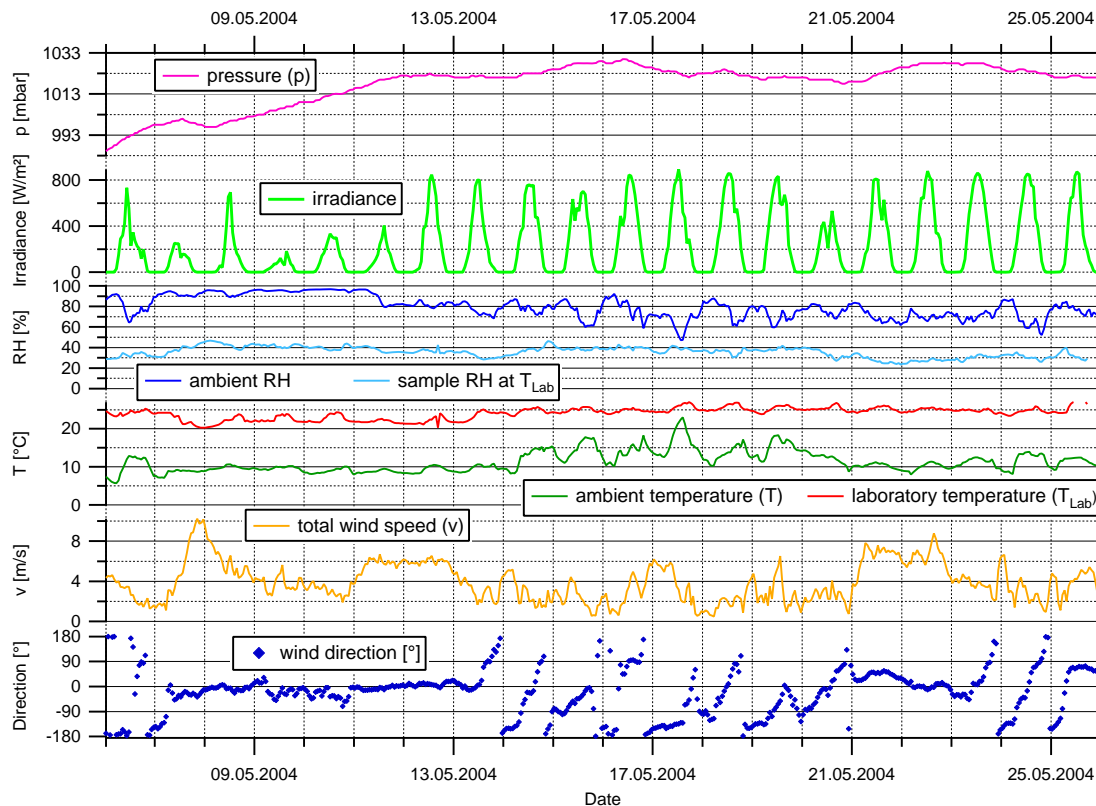
Fig. 1. Meteorological Parameters (measured by the University of East Anglia). The temperature in the laboratory as well as the derived sample RH at this temperature are also given.

Fig. 2. 5-day back trajectories (ECWMF).

EGU
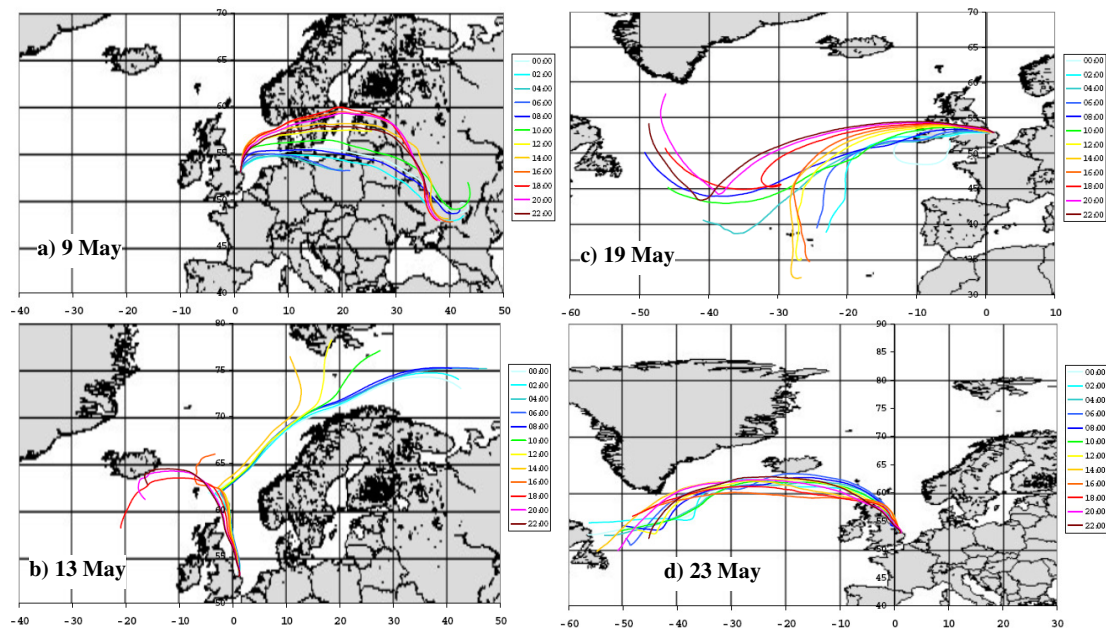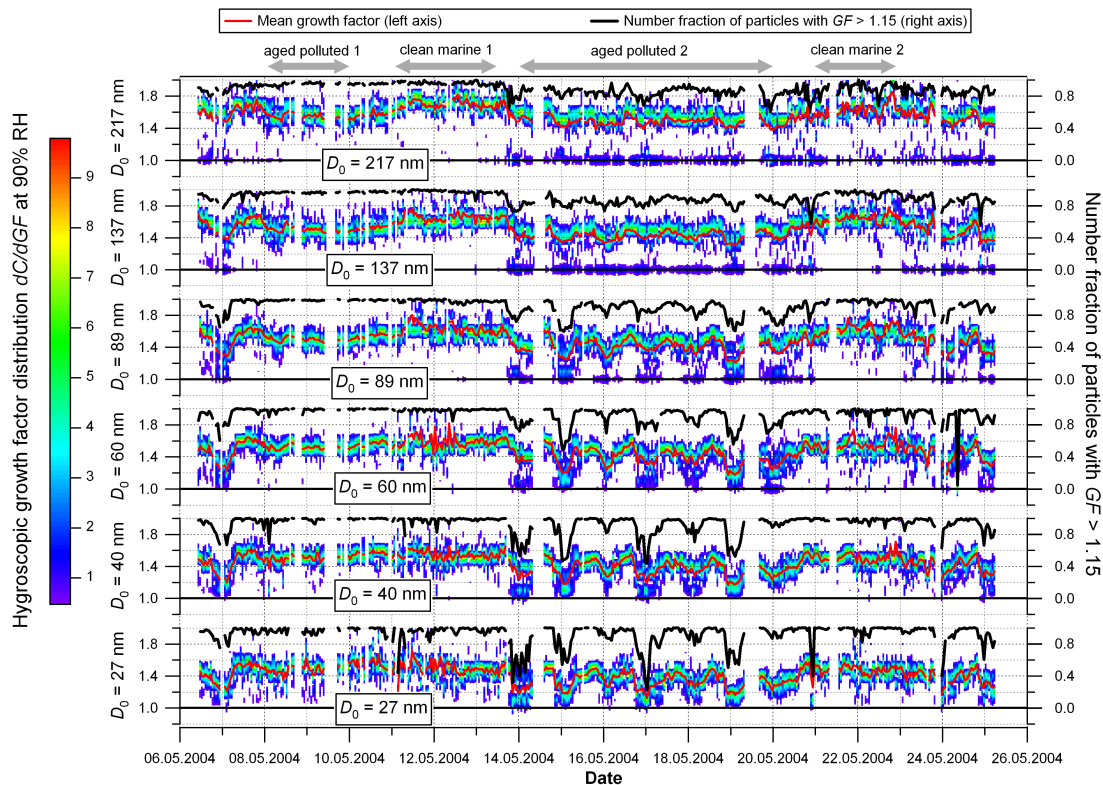
Fig. 3. Growth factor probability distributions for different particle dry sizes as measured with a HTDMA. The red lines represent the mean growth factors, black lines the number fraction of particles with $GF > 1.15$.
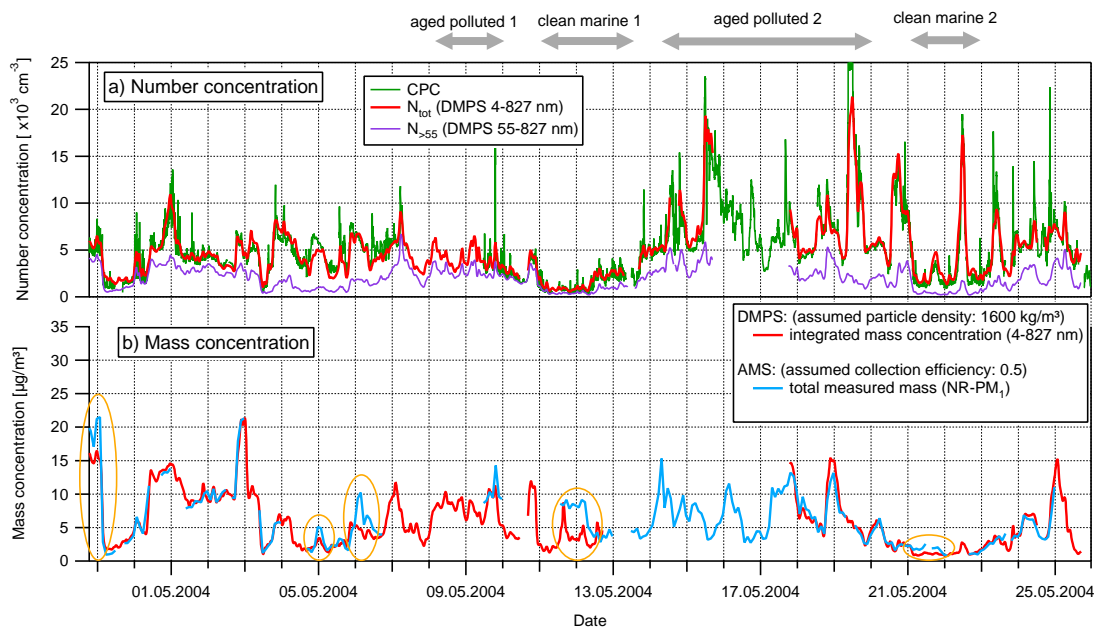
Fig. 4. Instrument comparison of number concentration from CPC and integrated DMPS **(a)** and mass loadings derived from DMPS and Q-AMS **(b)**. Orange circles indicate period where Q-AMS and DMPS disagree substantially. All disagreements occurred when the aerosol was either very acidic or had a high nitrate content, probably resulting in a higher collection efficiency of the Q-AMS. This means that the Q-AMS mass loadings are probably overcorrected in these periods by applying a collection efficiency of only 0.5 as has been done.

EGU
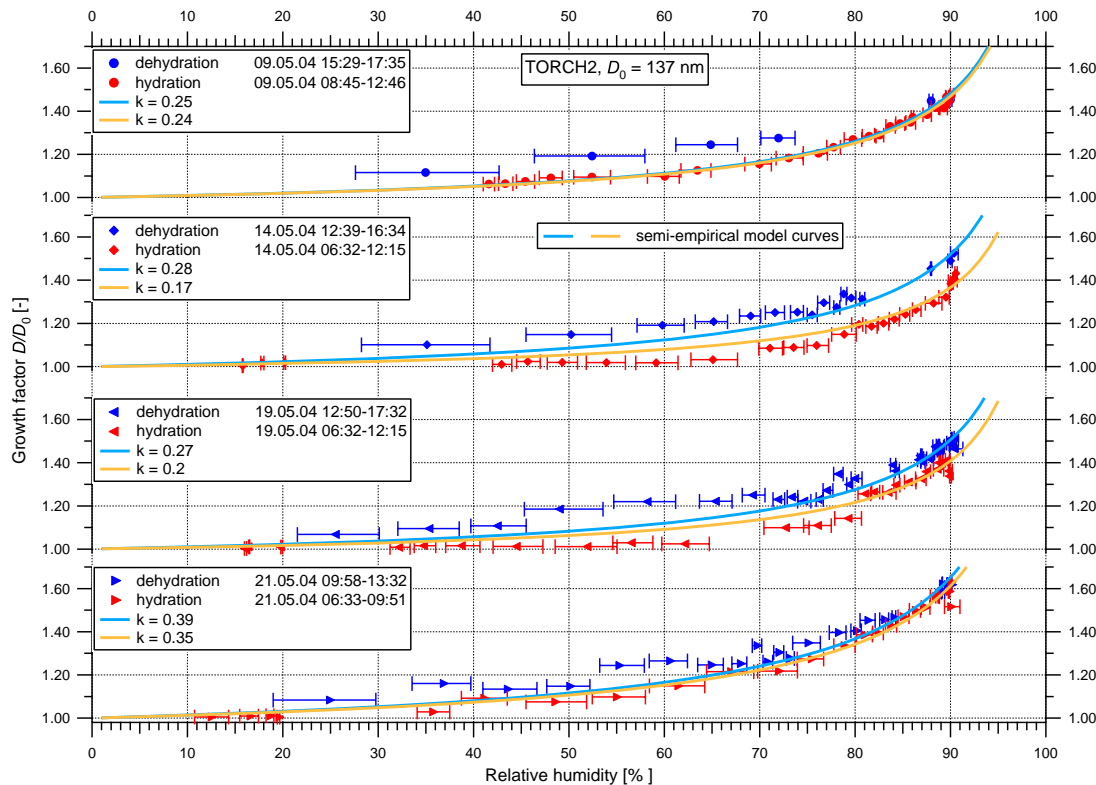
Fig. 5. RH-dependence of mean hygroscopic growth factors at hydration and dehydration as measured on four different days. Note that part of the difference between hydration/dehydration can be attributed to the changing aerosol composition/hygroscopicity during the measurement, as can be seen from the residual difference at 90% RH, where no hysteresis is to be expected. Error bars indicate the minimum and maximum RH in DMA2 during each scan. The semi-empirical model curves are fitted to the measurements at RH> 80%.

Title Page

Abstract Introduction

Conclusions References

Tables Figures

|◄ ►|

◄ ►

Back Close

Full Screen / Esc

Printer-friendly Version

Interactive Discussion

EGU

EGU
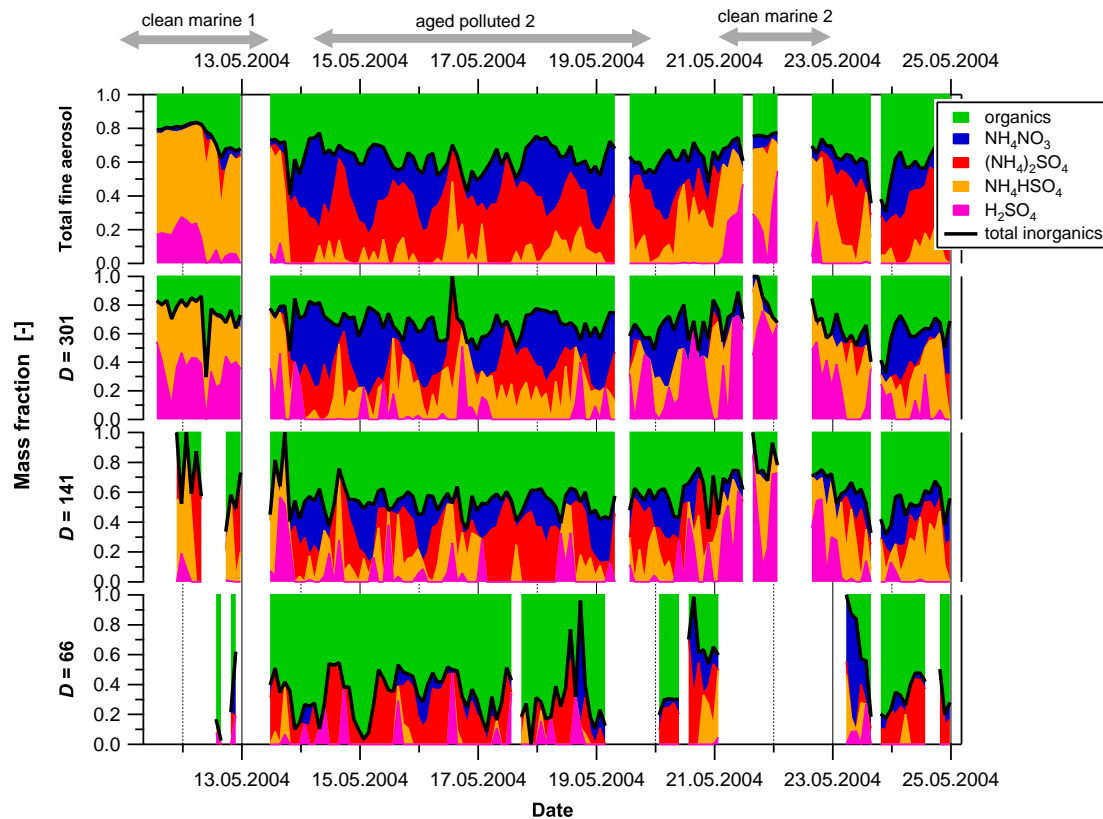
Fig. 6. Composition of non-refractory compounds as measured by the Q-AMS for the total fine aerosol and for different size ranges.

EGU
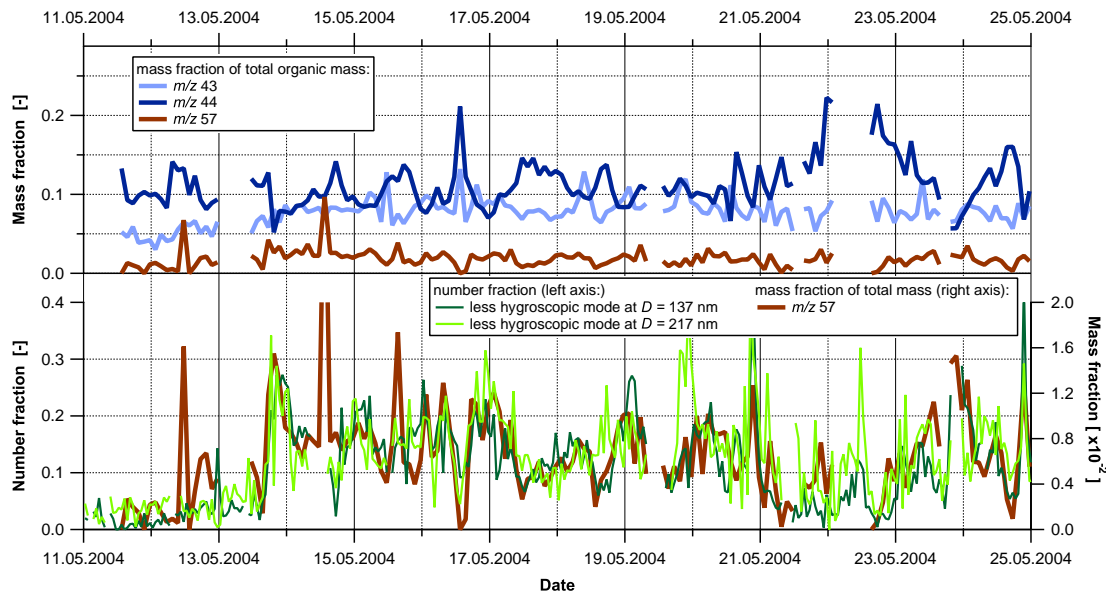
Fig. 7. Time series of key organic fragments and number fraction of particles in less hygroscopic mode.
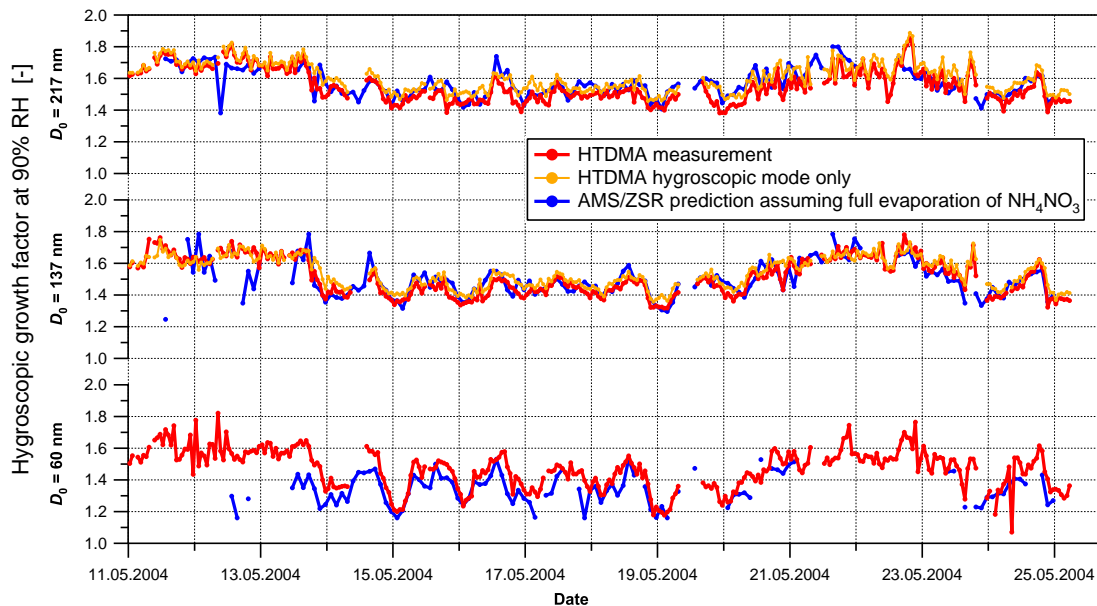
Fig. 8. Size-resolved hygroscopicity closure between HTDMA measurement and growth factor predictions using the ZSR relation with chemical composition according to Q-AMS data.

EGU
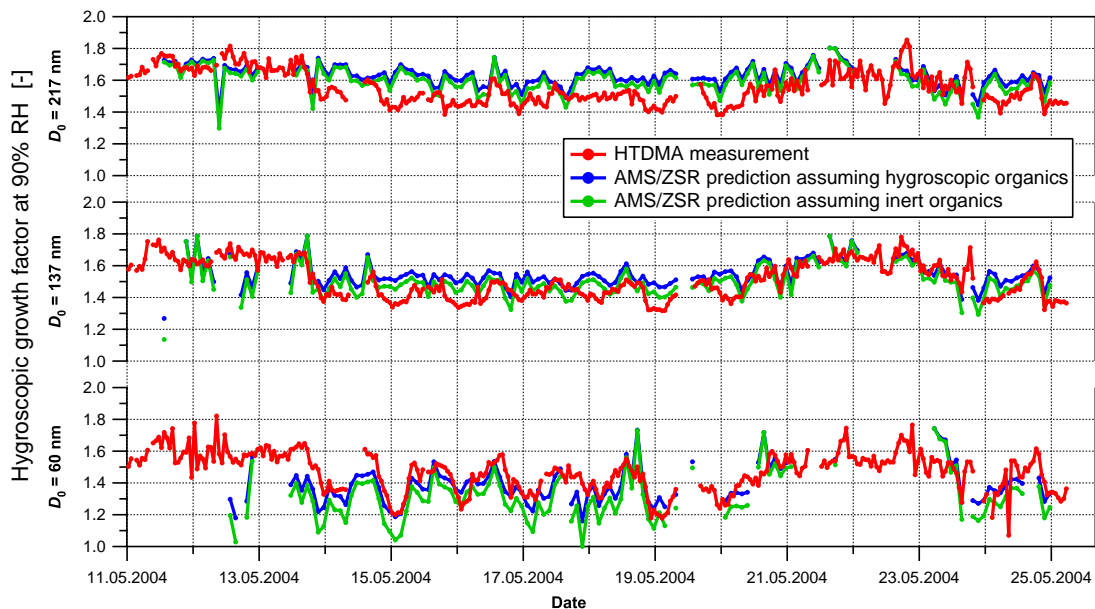
Fig. 9. Scatter plot of AMS/ZSR prediction versus HTDMA measurements for different model assumptions ("columns") and dry sizes ("rows"). The colour code of the data points indicates the measured nitrate mass fraction. Regression lines (blue) are fitted through the point (1.0, 1.0).

EGU

Fig. 10. Size-resolved hygroscopicity closure between HTDMA measurement and growth factor predictions using the ZSR relation with chemical composition according to Q-AMS data *including the assumption that all* NH_4NO_3 *was lost prior to HTDMA measurement.*
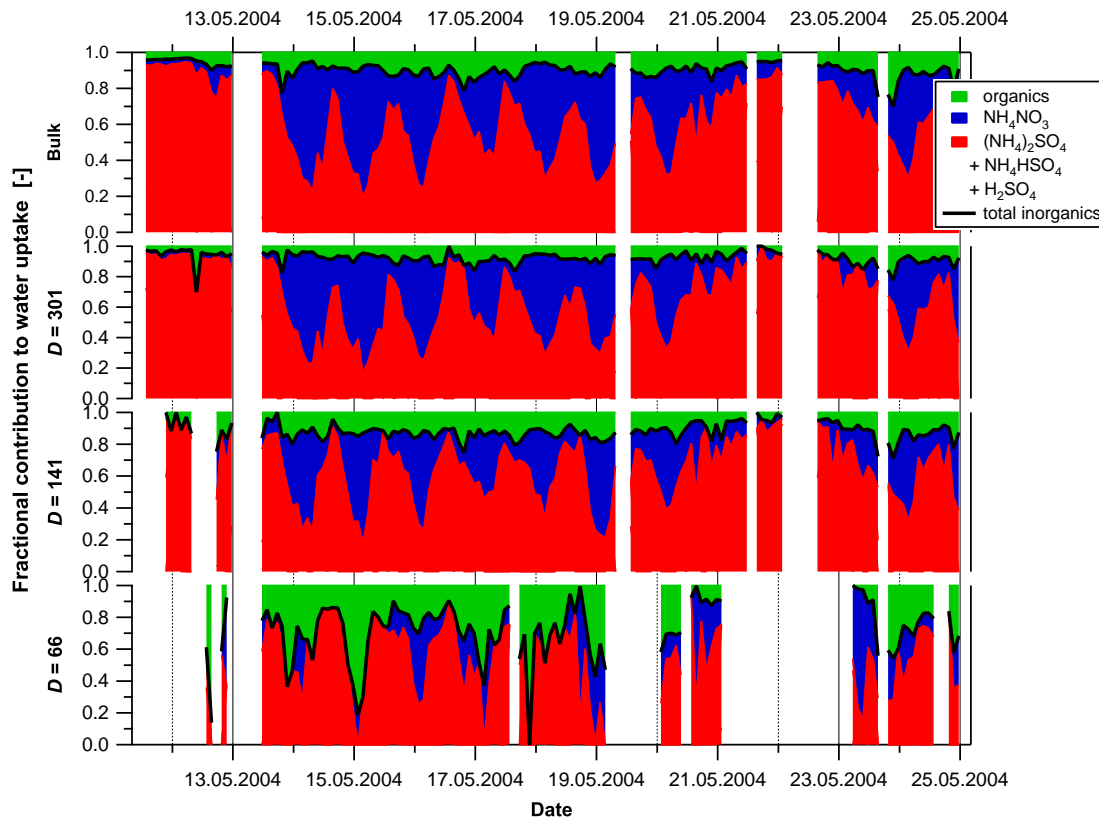
Fig. 11. Fractional contribution of major compounds to hygroscopic water uptake at 90% RH as calculated from the Q-AMS chemical composition. Total fine aerosol **(a)**, and particles with dry mobility diameters of around 301 **(b)**, 141 **(c)**, and 66 nm **(d)**.

EGU